MATEC Web of Conferences **14**, 15002 (2014)
DOI: 10.1051/matecconf/20141415002


# Creep behavior of a novel Co-Al-W-base single crystal alloy containing Ta and Ti at 982 °C

Fei Xue[1], Haijing Zhou[2], Xuhua Chen[1], Qianying Shi[1], Hai Chang[2], Meiling Wang[2], Xianfei Ding[2], and Qiang Feng[1,2,a]

[1] State Key Laboratory for Advanced Metals and Materials, University of Science and Technology Beijing, Beijing 100083, China
[2] National Center for Materials Service Safety, University of Science and Technology Beijing, Beijing 100083, China

**Abstract.** The tensile creep behavior of a Co-Al-W-base single crystal alloy containing Ta and Ti was investigated at 982 °C and 248 MPa. The lattice misfit of experimental alloy was measured to be positive by synchrotron X-ray diffraction at high temperature, and long term heat treatment at 1000 °C for 1000 h revealed a $\gamma'$ volume fraction of 75% without secondary phases. The creep test indicated that the creep properties of experimental alloy exceeded commercial 1st generation Ni-base single crystal superalloy CMSX-3 with respect to the rupture life. The initial cuboidal $\gamma'$ precipitates directionally coarsened parallel to the applied stress axis during the creep process. The stacking faults in {111} planes within $\gamma'$ rafts were the primary creep deformation mode by TEM investigation.

## 1. Introduction

Nickel-base superalloys strengthened by $L1_2$ type $\gamma'$ precipitates have been utilized in gas turbine applications for decades due to their superior creep resistance at high temperature [1,2]. The recently reported Co-Al-W-base alloys exhibited similar $\gamma$–$\gamma'$ two-phase microstructure and comparable creep properties to 1st generation Ni-base single crystal superalloy at 900 °C, serving as promising candidates for high temperature applications [3–5].

For an attempt to increase the $\gamma'$ solvus temperature, which was highly responsible for improving high temperature strength in $\gamma$–$\gamma'$ two-phase alloys, various alloying additions have been investigated in Co-Al-W-base alloys [6–9]. It was in general consistent that $\gamma'$ solvus temperature was significantly increased by Ta, Ti and Nb additions, and reduced by Fe and Cr additions to different extents, whereas controversial results were observed in quaternary alloys with the additions of Mo and V [6–9]. Later, several alloys with more complex compositions were developed, and further improvement in $\gamma'$ solvus temperature was evident in certain alloys [9]. However, the detrimental microstructural stability by the formation of secondary phases that enriched in refractory alloying elements was observed among most of these alloys due to the very narrow $\gamma$–$\gamma'$ two-phase region [4,6–8]. It appeared that only quaternary alloys containing Ta or Ti promoted microstructural stability, in addition to higher $\gamma'$ solvus temperature [4,6–8].

In contrast to the extensive microstructural studies, relatively limited work was conducted to investigate high temperature mechanical properties in Co-Al-W-base alloys, in particular for creep properties of single crystal alloys [4–6,10]. Compression and creep tests revealed a pronounced increase of high temperature strength by Ta addition, whereas quaternary alloys containing Ti yielded the best creep resistance [4–6,10]. All these investigations suggested that the improved high temperature strength was closely related to the $\gamma'$ solvus temperature and microstructural stability [4–6,10]. However, the creep tests were mainly performed within a relatively narrow range of temperatures from 850 to 950 °C due to the limitation of $\gamma'$ solvus temperature [4,10]. There was only few work involving creep properties at 1000 °C and 137 MPa, which was considered as high temperature and low stress in Co-Al-W-base single crystal alloys compared to Ni-base superalloys [5]. Furthermore, the studies on microstructural evolution and dislocation substructure during creep were limited, whereas the fundamental understanding of deformation behavior was crucial to increase the creep resistance of Co-Al-W-base alloys.

In our previous investigation, a Co-Al-W-Ta-Ti base alloy exhibited a high $\gamma'$ solvus temperature of 1131 °C and a $\gamma'$ volume fraction of approximately 63% at 1050 °C for 1000 h, indicating better microstructural stability than quaternary alloys containing Ta or Ti [11]. In this study, the creep behavior of the Co-Al-W-Ta-Ti base single crystal alloy was investigated at 982 °C and 248 MPa (high temperature and high stress), in comparison with the 1st and 2nd generation Ni-base single crystal superalloys. The associated long term microstructural stability and lattice misfit was also studied. The preliminary TEM investigation of the dislocation substructure has been performed to understand the deformation mechanism.

[a] Corresponding author: qfeng@skl.ustb.edu.cn

## 2. Experimental procedures

The nominal composition of the experimental alloy was Co-7Al-8W-1Ta-4Ti (at.%) and abbreviated as Alloy TaTi hereafter according to alloying elements. The single crystal bars with 15 mm in diameter and 150 mm in length were directionally solidified using Bridgman method at the Beijing Institute of Aeronautical Materials.

After single crystal bars were placed in quartz tubes back-filled with Ar gas, they were solution heat-treated at 1270 °C for 24 h and subsequently aged at 900 °C for 50 h. The creep specimens with a 25 mm gage length and a diameter of 5 mm were machined from the heat treated bars. The creep tests were conducted at 982 °C and 248 MPa, and the interrupted creep test was performed after the creep strain reached approximately 1% to investigate dislocation substructure. The crystal orientations of creep specimens were determined by using the Laue back reflection X-ray technique, and they were 4.7° and 5.5° away from [001] for the creep rupture and interrupted tests, respectively. All the creep tests were performed in air.

Microstructural observation was carried out using a ZEISS SUPRA 55 field-emission scanning electron microscope (FE-SEM) in secondary electron (SE) and back-scattered electron imaging (BSE) modes. The BSE mode was used to differentiate between the dendrite cores and interdendritic regions. It should be noted that the microstructure in this paper were taken in the dendrite cores. The $\gamma'$ volume fraction was measured by the standard point count method. For each alloy, three to five measurements were made to obtain sufficient statistics. A JEOL JEM-2100 transmission electron microscope was used for dislocation analyses. Discs with 0.20 mm in thickness and 3 mm in diameter were cut from the specimens after the interrupted creep test. The discs were mechanically polished and then subjected to twin-jet electropolishing in a solution of methanol with 10% volume fraction perchloric acid at −25 °C and 24 V. The lattice constants of $\gamma$ and $\gamma'$ phases were determined by synchrotron X-ray diffraction (XRD) using BL14B1 at the Shanghai Synchrotron Radiation Facility (SSRF). The results of diffraction patterns were analyzed with the Jandel Scientific PeakFit computer program.

## 3. Results

### 3.1. As cast and heat treated microstructure

The average primary dendrite arm spacing was measured to be $296 \pm 11\ \mu$m. The eutectic pools were completely dissolved and the dendritic segregation was reduced by solution treatment, although some residual segregation remained since the dendritic pattern was still evident by etching. Figure 1a shows the typical $\gamma/\gamma'$ two-phase microstructure after solution treatment and aging treatment at 900 °C for 50 h. The $\gamma'$ precipitates exhibited cuboidal morphology with the volume fraction of $\sim$ 87% and the mean size of $\sim$0.21 $\mu$m. In addition to $\gamma$ and $\gamma'$ phases, no secondary phases were observed except for limited amount of MC carbides in the interdendritic region. Figure 1b exhibits the typical microstructure after long term heat

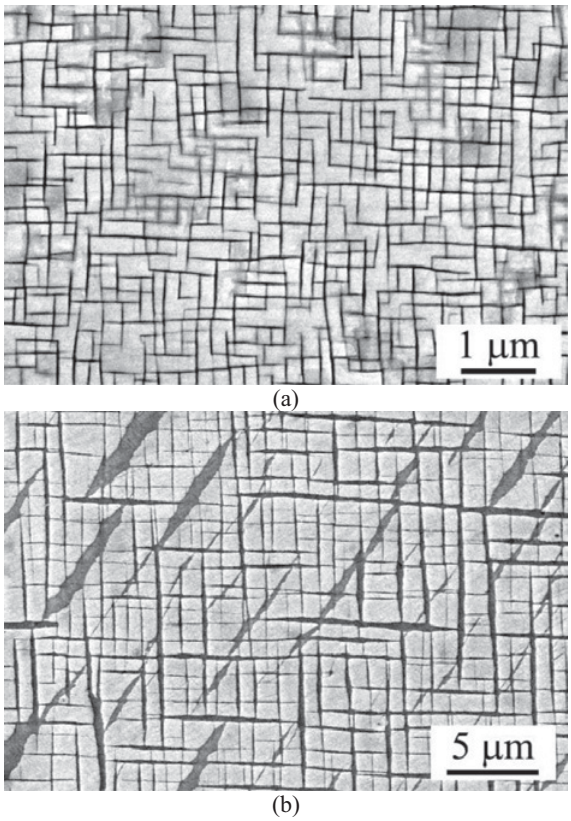


**Figure 1.** Typical microstructure of Alloy TaTi after solution treatment at 1270 °C for 24 h and aging at (a) 900 °C for 50 h and (b) 1000 °C for 1000 h.

treatment at 1000 °C for 1000 h, which was performed on the purpose of evaluating microstructural stability. The $\gamma/\gamma'$ two-phase micro-structure still existed with cuboidal $\gamma'$ precipitates accounting for 75% volume fraction, and no secondary phases was observed in the matrix.

Figure 2 is (004) diffraction pattern of an undeformed specimen of aged Alloy TaTi by using synchrotron X-ray diffraction technique at 1000 °C. Two separated peaks were obviously derived from the raw data, and the right peak with relative high intensity was expected to be $\gamma'$ phase due to its high volume fraction at this temperature (Fig. 1b). Therefore, the lattice constant of $\gamma$ and $\gamma'$ phases were measured to be 0.3641 and 0.3657 nm, respectively, resulting in a positive lattice misfit of + 0.44% for Alloy TaTi at 1000 ° C.

### 3.2. Creep behavior

Figure 3a shows creep curves of Alloy TaTi at 982 °C and 248 MPa, and it also includes commercial 1st and 2nd generation Ni-base single crystal superalloys CMSX-3 and CMSX-4 for comparison, respectively [12]. The creep rupture life of Alloy TaTi was 122.0 h, which falls somewhere between CMSX-3 (90.1 h) and CMSX-4 (178.0 h). Additionally, Alloy TaTi processed the best ductility with a large rupture strain of approximately 40%. The expanded creep curves within 1% strain of Alloys TaTi, CMSX-3 and CMSX-4 are shown in Fig. 3b. In contrast to the creep rupture life, Alloy TaTi exhibited a 1% creep time of approximately 25 h, inferior than

**Table 1.** Creep properties of Alloy TaTi and Ni-base single crystal superalloys CMSX-3 and CMSX-4 at 982 °C and 248 MPa.

| **Alloy** | Rupture time, h | 1% creep time, h | Min. creep rate, $10^{-9}$ $s^{-1}$ | Elonga-tion, % |
|---|---|---|---|---|
| Alloy TaTi | 122.0 | 24.9 | 1.1 | 39.5 |
| CMSX-3 [12] | 90.1 | 35.1 | 58.9 | 24.5 |
| CMSX-4 [12] | 178.0 | 77.5 | 9.4 | 26.8 |

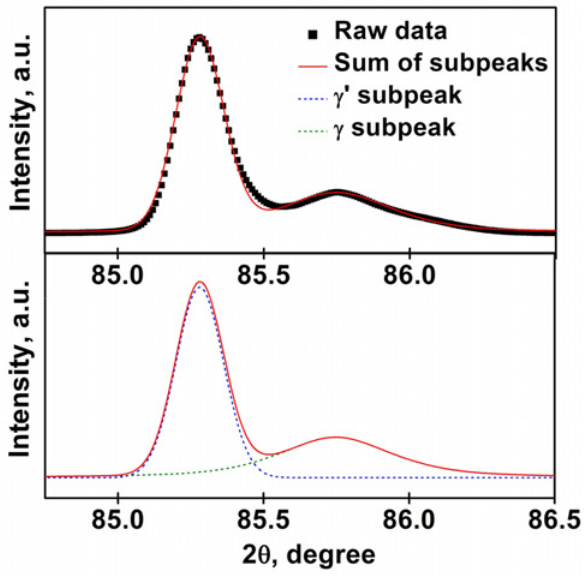


**Figure 2.** (004) diffraction pattern of an undeformed specimen of single crystal Alloy TaTi by using synchrotron X-ray diffraction technique at 1000 °C. The fitted sub-peaks of $\gamma$ and $\gamma'$ are shown in the plot.

both CMSX-3 and CMSX-4. Figure 3b also shows the interrupted 1% creep curve of Alloy TaTi, which presented very analogous creep behavior to the rupture test.

Figure 3c illustrates the creep rate curve of Alloy TaTi and the right inset is the enlarged curve at time ranged from 0 to 20 h, showing typical three stages of creep. A brief primary transient where the strain rate decreased rapidly was initially present, without a well-defined steady state stage, it was then immediately followed by a gradual increase in strain rate. The minimum creep rate of the experimental alloy between the primary transient and accelerating stage was measured to be $1.1 \times 10^{-9}$ $s^{-1}$, which is an order of magnitude less than CMSX-3 ($5.9 \times 10^{-8}$ $s^{-1}$) and even superior to CMSX-4 ($9.4 \times 10^{-9}$ $s^{-1}$) in the same order. However, it took about 4 h to reach the minimum strain rate for Alloy TaTi, whereas it was near 10 h and 16 h for CMSX-3 and CMSX-4, respectively. Table 1 lists the creep property of Alloy TaTi and Ni-base single crystal superalloys CMSX-3 and CMSX-4 at 982 °C and 248 MPa [12].

### 3.3. Crept microstructure and submicrostructure

In order to illustrate the deformation mechanism of Alloy TaTi at 982 °C, microstructure was examined after the rupture test and the interrupted creep test with the ∼1% plastic strain.

Figures 4a and 4b are SEM images, showing the typical microstructures of Alloy TaTi after the interrupted and rupture creep tests at 982 °C and 248 MPa, respectively. The directionally coarsened $\gamma'$ rafts parallel to the applied tensile stress was exhibited after the interrupted test with 1.1% plastic strain for 26 h (Fig. 4a). In comparison to $\gamma'$ rafts in the gauge section, no rafting behavior and less coarsened $\gamma'$ precipitates was evident in the button head of the interrupted specimen (image not shown), indicating significant coarsening induced by plastic deformation. More irregular $\gamma'$ plates and rafts with considerable coarsening were observed after the failure at 122.0 h with near 40% strain shown in Fig. 4b. It should be noted that the microstructure after creep rupture test was taken 10 mm away from the necked region.

Figure 5 presents the bright-field transmission electron micrographs showing Alloy TaTi with 1.1% creep strain in 26 h at 982 °C and 248 MPa from the (001) and (011) zone axis. It should be mentioned that micrographs of Figs. 5a and b were taken from the foils which were normal to [001] and [111] orientations, respectively. The observation from the [001] zone axis showed that an appreciable density of stacking faults existed in the $\gamma'$ lamellae, whereas limited dislocations were observed in the $\gamma$ channel. The stacking faults were parallel to two different $< 110 >$ directions as marked in Fig. 5a. From the [011] zone axis, four sets of stacking faults were evident in the $\gamma'$ lamellae and marked as A, B, C and D in Fig. 5b. The lines A and B appeared in an edge-on view, indicating that they were stacking faults on different {111} planes. The stacking faults C and D were also expected to be on different planes because of their different directions, and D might be on the plane parallel to the foil due to its larger area.

## 4. Discussion

### 4.1. $\gamma'$ morphology and $\gamma$-$\gamma'$ lattice misfit

It has been revealed that the directional coarsening behavior of $\gamma'$ precipitates during high temperature creep was resulted from the superposition of the $\gamma$-$\gamma'$ lattice misfit and applied stresses in Ni-base superalloys [13]. The investigation of Fährmann and coworkers indicated that the initial cuboidal $\gamma'$ precipitates evolved to plates aligned parallel to the tension axis and perpendicular to the compression axis for Ni-Al-Mo alloy with the positive misfit at elevated temperature [14].

In the current study, analyses of the lattice constant demonstrated the positive misfit at 1000 °C in Alloy TaTi, and $\gamma'$ rafts were parallel to the applied tensile stress axis during creep at 982 °C. Both results are consistent, again indicating the raft behavior associated with the positive lattice misfit and the applied tensile stress during creep process. This raft behavior was very

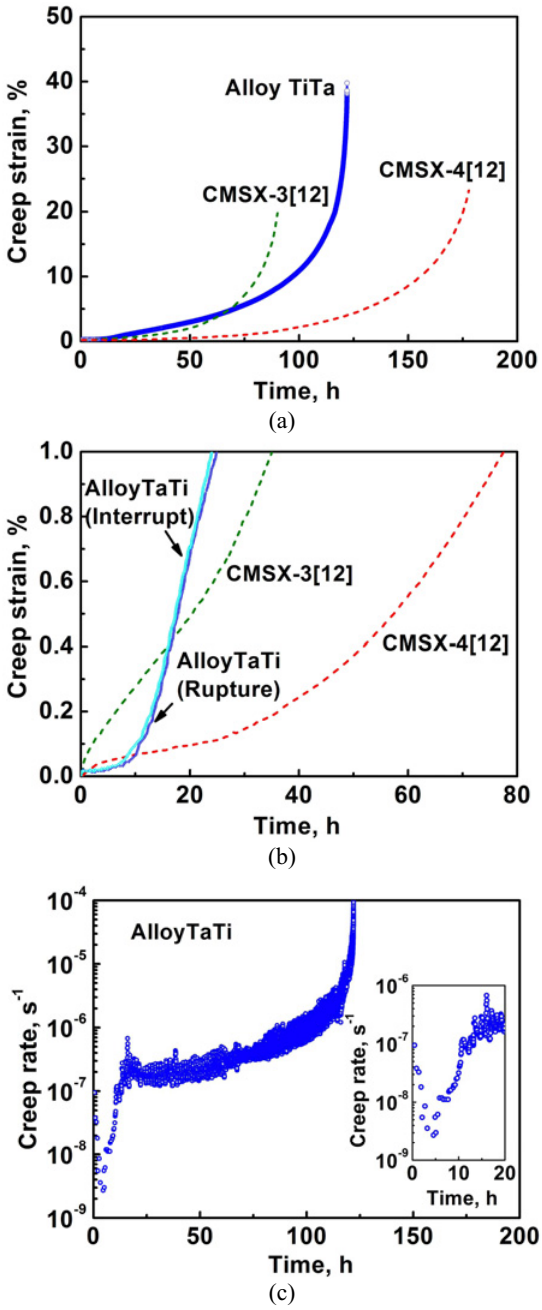


**Figure 3.** Creep behavior of single crystal Alloy TaTi and Ni-base single crystal superalloys CMSX-3 and CMSX-4 [12] at 982 °C and 248 MPa. (a) creep curve, (b) expanded 1% creep curve and (c) creep rate vs time.

analogous to other investigated Co-Al-W-base alloys during creep [4,9,15,16].

The positive lattice misfit of Alloy TaTi appears to be resulted from its chemical composition and elemental partitioning behavior. Alloying elements Ta and Ti, with an atomic radius relatively larger than Co, were experimentally determined to preferentially partition into $\gamma'$ phase [7], which in turn should possess an higher lattice constant than $\gamma$ phase. Similar to the chemical composition of the present alloy TaTi, Pollock and coworkers also utilized the partition behavior of Ta and Ti on the purpose

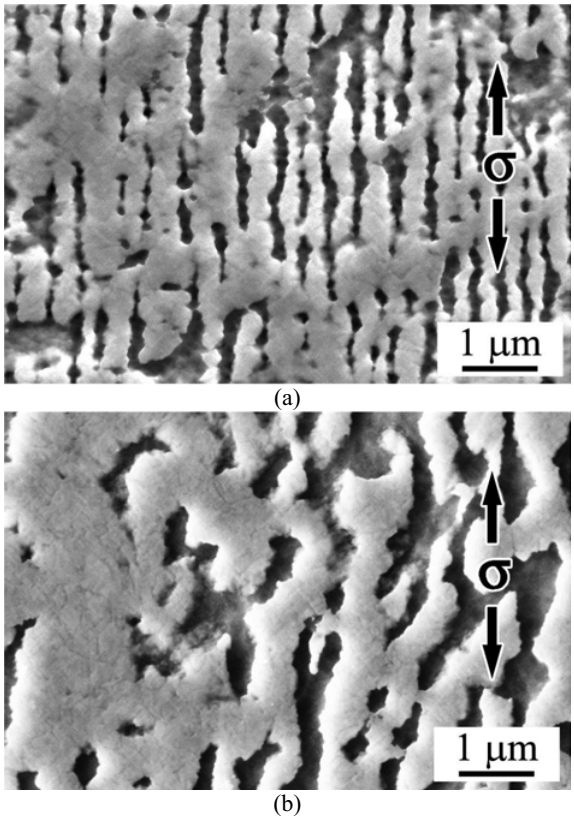


**Figure 4.** Typical microstructure in the dendritic region of aged Alloy TaTi after (a) interrupted creep test with 1.1% strain and (b) creep rupture at 982 °C and 248 MPa . Stress axis is vertical. Noting that (a) and (b) was taken in the gauge section and 10 mm away from the necked region, respectively.

to yield the positive misfit in Ni-base superalloys PWA at high temperature [13].

### 4.2. Creep behavior

To date, the investigation of creep behavior was limited in Co-Al-W-base alloys, whereas majority of studies were focused on the fundamental understanding of microstructural stability. Although series compressive creep tests were conducted in polycrystalline alloys, the tensile creep properties of single crystal alloys that are crucial to the potential application as the blade alloy were less reported [5,9,10,16]. Moreover, the creep behavior was mainly investigated at 850 to 950 °C due to the microstructural stability of Co-Al-W-base alloys, but the information about higher temperature creep resistance was very limited, especially under high stress level [5,16].

In the current study, the high temperature creep behavior was investigated at 982 °C and 248 MPa, a typical creep condition for Ni-base single crystal superalloys. Figure 6 shows creep properties of Alloy TaTi and other reported Co-Al-W-base alloys using Larson Miller parameter, including commercial Ni-base single crystal superalloys CMSX-3, CMSX-4 and CMSX-10 [17,18]. Since these creep tests were conducted at various stresses, the direct comparison of Larson Miller parameter is not available, whereas several characteristics can be drawn from Fig. 6. Alloy TaTi is clearly superior to CMSX-3, a

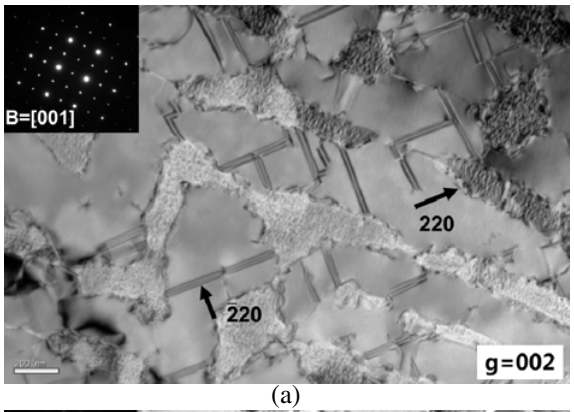


(a)

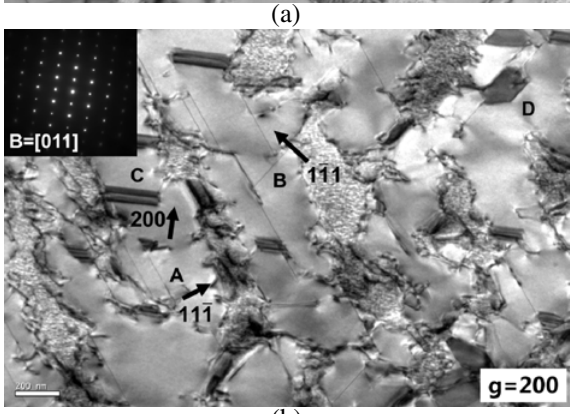


(b)

**Figure 5.** Bright-field transmission electron micrographs showing Alloy TaTi after 1.1% creep strain in 26 h at 982 °C and 248 MPa from (a) the [001] and (b) [011] zone axis.

typical 1st generation Ni-base single crystal superalloys, and appeared to approach CMSX-4. It should be noted that the chemical composition of Alloy TaTi is quite simple compared with CMSX-3, indicating high potential improvement by high-order alloying. In comparison with other Co-Al-W-base alloys, Alloy TaTi is superior to ternary and quaternary alloys containing Ta which are inferior or comparable to CMSX-3, and Alloy TaTi is somewhat similar to 6Ti alloy (Fig. 6). The improvement is expected to be associated with the increase of $\gamma'$ solvus temperature that featured the early development of Ni-base superalloys represented by Nimonic series of alloys [1]. The $\gamma'$ solvus temperature of Alloy TaTi was 1131 °C [11], exhibiting ∼100 °C greater than ternary alloy and ∼50 °C higher than quaternary alloys containing Ta or Ti [4,5]. Another reason for improving the creep resistance of the experimental alloy might be its high temperature stability as the volume fraction of $\gamma'$ precipitates was 75% even after aging at 1000 °C for 1000 h (Fig. 1b). This is consistent with previous investigations, which suggested that Co-Al-W-base alloys with $\gamma'$ volume fraction more than 60% and near 75% exhibited better tensile and creep strength, respectively [16,19].

In order to understand the creep behavior of the experimental alloy, the microstructural evolution and creep mechanism need to be considered. The high temperature creep (more than 1000 °C) behavior of Ni-base single crystal superalloys with high $\gamma'$ volume fraction was well investigated [20]. During the early stage, $\gamma'$ precipitates

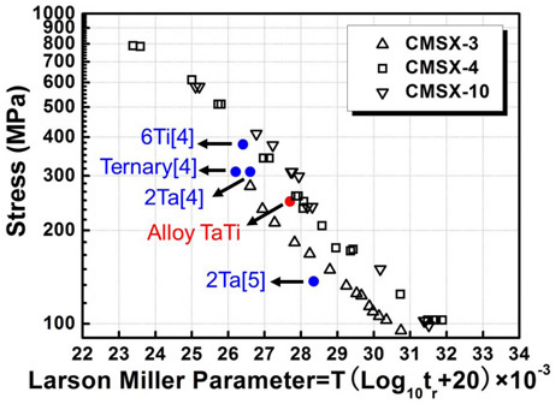


**Figure 6.** Stress vs. Larson Miller parameter of experimental alloy. Co-Al-W-base and commercial Ni-base single crystal superalloys are also included [17,18].

were cuboidal and inhomogeneous deformation occurred by the cross slip of dislocations in $\gamma$ matrix channels. After the rafting was complete, the matrix channels no longer produced a continuous path for dislocation motion that was necessary for gradual deformation, and it thus resulted in the shearing of the $\gamma'$ phase by paired dislocations [20]. In the current study, the observation of dislocation substructure revealed planar defects in $\gamma'$ rafts, suggesting a shearing mechanism rather than a bypassing mechanism. This mechanism is consistent with ternary and quaternary alloys containing Ta after creep deformation at 850 °C and 1000 °C, respectively [5,15]. It is also similar to Ta-containing alloy during compressive deformation when 1/3<112> partial dislocations slip with a high density of stacking faults in the $\gamma'$ precipitates at 980 ∼ 1000 °C [6]. This deformation mechanism effectively sustained high temperature strength for Ta-containing alloy compared to the ternary alloy with rapid decrease in the flow stress due to 1/2 <110> dislocations by-passing the $\gamma'$ precipitates [6]. The current creep test at 982 °C is in the high temperature range of Co-Al-W-base alloy as it is approximately 150 °C below the $\gamma'$ solvus temperature, but the reason why the shearing of $\gamma'$ rafts by partial dislocations coupled with stacking faults was not understood yet. More work is required to clarify the change of stacking fault energy by additions of Ta and Ti.

The current study indicates that both high $\gamma'$ solvus temperature and high $\gamma'$ volume fraction contributed to improving high temperature creep resistance of a Co-Al-W-base alloy containing Ta and Ti. The deformation microstructure dominated by stacking faults might also be beneficial to the creep strength at high temperature. Potential improvement is expected since this class of new Co-base alloys is in its early stage.

## 5. Conclusions

The high temperature creep behavior of a Co-Al-W-Ta-Ti alloy was investigated in the current study. The following conclusions can be drawn:

1. By using synchrotron radiation, the lattice misfit of the experimental alloy was determined to be $+\ 0.444\%$ at 1000 °C.
2. The creep rupture time of the experimental alloy was superior to 1st generation Ni-base single crystal superalloys CMSX-3 at 982 °C and 248 MPa.
3. Directional coarsening of initial cuboidal $\gamma'$ precipates occurred during creep and promoted the formation of $\gamma'$ rafts parallel to the applied tensile stress, suggesting good consistence with its positive misfit at 1000 °C.
4. During creep process, the dislocations accompanied with stacking faults existed in the $\gamma'$ rafts, indicating that the shearing of $\gamma'$ precipitates occurred.

The authors are grateful for the support of the National Natural Science Foundation of China (Grant No. 50771012, 51301014 and 51201006) and Aviation Science Foundation of China (Grant No. 2009ZF74011).

## References

[1] R.C. Reed, *The superalloys: fundamentals and applications*, (Cambridge University Press, Cambridge, 2006)
[2] T.M. Pollock, S. Tin, J. Propul. Power, 22, 361 (2006)
[3] J. Sato, T. Omori, K. Oikawa, I. Ohnuma, R. Karinuma, K. Ishida, Science, **312**, 90 (2006)
[4] M.S. Titus, A. Suzuki, T.M. Pollock, in: E.S. Huron, R.C. Reed, M.C. Hardy, M.J. Mills, R.E. Montero, P.D. Portella, J. Telesman (Eds.) *Superalloys 2012*, TMS, Champion, PA, 2012, pp. 823
[5] K. Tanaka, M. Ooshima, N. Tsuno, A. Sato, h. Inui, Philos. Mag., 1 (2012)
[6] A. Suzuki, T.M. Pollock, Acta Mater., **56**, 1288 (2008)
[7] T. Omori, K. Oikawa, J. Sato, I. Ohnuma, U.R. Kattner, R. Kainuma, K. Ishida, Intermetallics, **32**, 274 (2013)
[8] F. Xue, M. Wang, Q. Feng, in: E.S. Huron, R.C. Reed, M.C. Hardy, M.J. Mills, R.E. Montero, P.D. Portella, J. Telesman (Eds.) *Superalloys 2012*, TMS, Champion, PA, 2012, pp. 813
[9] A. Bauer, S. Neumeier, F. Pyczak, R.F. Singer, M. Gken, Mater. Sci. Eng., A, **550**, 333 (2012)
[10] A. Bauer, S. Neumeier, F. Pyczak, M. Gken, in: E.S. Huron, R.C. Reed, M.C. Hardy, M.J. Mills, R.E. Montero, P.D. Portella, J. Telesman (Eds.) *Superalloys 2012*, TMS, Champion, PA, 2012, pp. 695
[11] F. Xue, H.J. Zhou, X.F. Ding, M.L. Wang, Q. Feng, Mater. Lett., **112**, 215 (2013)
[12] G.L. Erickson, K. Harris, US Patent no. 4643782 (1987)
[13] T.M. Pollock, A.S. Argon, Acta. Metall. Mater., **42**, 1859 (1994)
[14] M. Fahrmann, W. Hermann, E. Fahrmann, A. Boegli, T.M. Pollock, H.G. Sockel, Mater. Sci. Eng., A, **260**, 212 (1999)
[15] F. Pyczak, A. Bauer, M. Gken, S. Neumeier, U. Lorenz, M. Oehring, N. Schell, A. Schreyer, A. Stark, F. Symanzik, Mater. Sci. Eng., A, **571**, 13 (2013)
[16] M.S. Titus, A. Suzuki, T.M. Pollock, Scr. Mater., **66**, 574 (2012)
[17] J.R. Davis, *Heat-resistant materials*, (ASM International, 1997)
[18] G.E. Fuchs, J Mater. Eng. Perform., **11**, 19 (2002)
[19] K. Shinagawa, T. Omori, K. Oikawa, R. Kainuma, K. Ishida, Scr. Mater., **61**, 612 (2009)
[20] T.M. Pollock, R.D. Field, Chapter 63 Dislocations and high-temperature plastic deformation of superalloy single crystals, in: F.R.N. Nabarro, M.S. Duesbery (Eds.) *Dislocations in Solids*, Elsevier, 2002, pp. 547